Accurate Anchor Free Tracking

Shengyun Peng
College of Civil Engineering
Tongji University
Shanghai, P.R. China

1553983@tongji.edu.cn

Yunxuan Yu
Electrical and Computer
Engineering Department, UCLA
Los Angeles, USA

yunxuan.yu@hotmail.com

Kun Wang
Electrical and Computer
Engineering Department, UCLA
Los Angeles, USA

wangk@ucla.edu

Lei He
Electrical and Computer
Engineering Department, UCLA
Los Angeles, USA

lhe@ee.ucla.edu

Abstract

Visual object tracking is an important application of computer vision. Recently, Siamese based trackers have achieved a good accuracy. However, most of Siamese based trackers are not efficient, as they exhaustively search potential object locations to define anchors and then classify each anchor (i.e., a bounding box). This paper develops the first Anchor Free Siamese Network (AFSN). Specifically, a target object is defined by a bounding box center, tracking offset and object size. All three are regressed by Siamese network with no additional classification or regional proposal, and performed once for each frame. We also tune the stride and receptive field for Siamese network, and further perform ablation experiments to quantitatively illustrate the effectiveness of our AFSN. We evaluate AFSN using five most commonly used benchmarks and compare to the best anchor-based trackers with source codes available for each benchmark. AFSN is $3 \times -425\times$ faster than these best anchor based trackers. AFSN is also 5.97% to 12.4% more accurate in terms of all metrics for benchmark sets OTB2015, VOT2015, VOT2016, VOT2018 and TrackingNet, except that SiamRPN++ is 4% better than AFSN in terms of Expected Average Overlap (EAO) on VOT2018 (but SiamRPN++ is $3.9\times$ slower).

1. Introduction

Video object tracking, which locates an arbitrary object in a changing video sequence, powers many computer vision topics such as automatic driving and pose estimation. Liu *et al*. [27] focus on the task of searching a specific vehi-
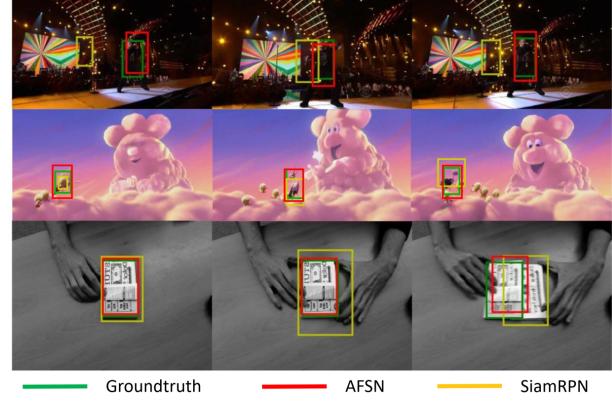

Figure 1. Comparisons of our tracker with SiamRPN. AFSN is able to resist the interference of similar objects, illumination variation, and predict a more precise bounding box than SiamRPN. When the ratio of length to width is abnormal, AFSN can still estimate the bounding box accurately.

cle that appears in the surveillance networks. Doellinger *et al*. [9] use tracking methods to predict local statistics about the direction of human motion. A core problem in tracking is how to locate an object accurately and efficiently in challenging scenarios like background clutter, occlusion, scale variation, illumination change, deformation and other variations [42].

Current trackers can be generally classified into two branches, *i.e.*, generative and discriminative methods. Generative methods [18, 28, 29, 38, 46] consider tracking as a reconstruction problem and they maintain a template set online to represent the moving target. Discriminative trackers like MOSSE [5], Struck [12], CSK [14], KCF [15] learn

a classifier between foreground and background [2, 1, 10]. Correlation filter (CF) trackers can update online with current video due to its high efficiency. However, a clear deficiency of using data derived exclusively from current video results in learning a comparatively simple model. In contrast, trackers based on deep neural network aim to make full use of the entire tracking dataset [31]. Siamese networks, which track an object through similarity comparison, have developed into various versions in the tracking community [4, 11, 25, 24, 13, 37, 39, 43, 40, 44].

Although these tracking approaches obtain balanced accuracy and speed, most of the successful Siamese trackers rely on the anchors generated before tracking. A tracking object is represented by an axis-aligned bounding box that encompasses the object. The localization of the object becomes an image classification of an extensive number of potential anchors. Since this method needs to enumerate all possible object locations and regress a normalized distance for each prospective bounding box, it is inefficient. Furthermore, it restricts the ability of proposing accurate bounding box when the ratio of length to width is abnormal.

To deal with this challenge, we propose the first tracker without using an anchor. First, our Anchor Free Siamese Network (AFSN) represents an object with merely a center point, a tracking offset and the object size. Compared with anchor-based trackers, it has a reduced complexity. Second, we model an object through the network inference result rather than modifying the object position and size with the bounding boxes proposed in advance. Only one estimation is conducted for each frame, with no need to classify each potential anchor. The inference efficiency is improved significantly. Third, our method leverages all images in the large scale supervised tracking datasets. Clearly, using videos from various categories can largely improve robustness. Ablation experiments also demonstrate the effectiveness of our AFSN.

To further improve the tracking quality, we test different network backbones. We find that the accuracy drops severely when the network backbone grows deeper. This problem has also been discovered in SiamDW [45]. One reason is that these deeper and wider network architectures are mainly designed for image classification tasks, but not necessarily are optimal for tracking. We also reveal that a bigger network stride improves overlap area of receptive fields for two neighboring output score maps, but reduces tracking position precision, so the network stride needs to be optimized. In order to take full advantage of modern deep neural networks, we in this paper train 8 different backbones considering stride, receptive field, group convolution and kernel size. Section 4 gives a further analysis on the backbone design. The resulting AFSN outperforms a state-of-the-art tracker SiamRPN, as illustrated in Fig. 1.

We evaluate the proposed method using most commonly used datasets including OTB2015 [42], VOT2015 [22], VOT2016 [19], VOT2018 [20] and TrackingNet [30]. Our AFSN can achieve leading performance in all of the 5 datasets. Compared with SiamRPN, AFSN increases the precision rate and success rate by 0.93% and 5.97% on OTB2015, respectively. In terms of EAO (expected average overlap), it outperforms SiamRPN on VOT2015, VOT2016 and VOT2018 by 0.381, 0.372 and 0.398, respectively. Meanwhile, AFSN runs at 136 FPS (frames per second) on Titan Xp.

The contributions of this paper can be summarized in three-fold as follows: 1) We propose the Anchor Free Siamese Network (AFSN), which is the first anchor free end-to-end tracker trained with large scale dataset. 2) A quantitative analysis of the network architecture, especially receptive field and network stride, leads to the best network backbone for our AFSN. 3) Our tracker AFSN has balanced accuracy and robustness for five commonly used datasets.

The rest of the paper is organized as follows. Section 2 introduces related work. Section 3 presents our AFSN, and Section 4 optimizes the network backbone. Section 5 performs experimental study, and Section 6 concludes the paper.

2. Related work

2.1. Trackers based on Siamese network

Recently, Siamese network has drawn widespread attention in tracking community because of its good accuracy and speed, and the capability to make full use of the tracking dataset during offline training. Basically, a Siamese network is used for comparing the exemplar and instance image pairs, and exporting the final results by a score map. SINT [37] proposes learning a generic matching function for tracking, which can be applied to new tracking videos of previously unseen target objects. GOTURN [13] adapts the Siamese network to tracking and utilizes fully connected layers as fusion tensors. SiamFC [4] introduces the correlation operator. Dense and efficient sliding window evaluation is achieved with a biliear layer that computes the cross correlation of its two inputs, namely instance branch and exemplar branch. SiamRPN [25] integrates a popular detection technique, namely region proposal network (RPN) with SiamFC. The tracker refines the proposal to avoid the expensive multi-scale tests. SiamRPN++ [24] is a ResNet-driven Siamese tracker, which performs layer-wise and depth-wise aggregations. However, a tracking object is represented by an axis-aligned bounding box that emcompasses the object. The localization of the object becomes an image classification of an entensive number of potential anchors. Since this method needs to enumerate all possible object locations and regress a normalized distance for all provective bounding boxes, sliding window based object
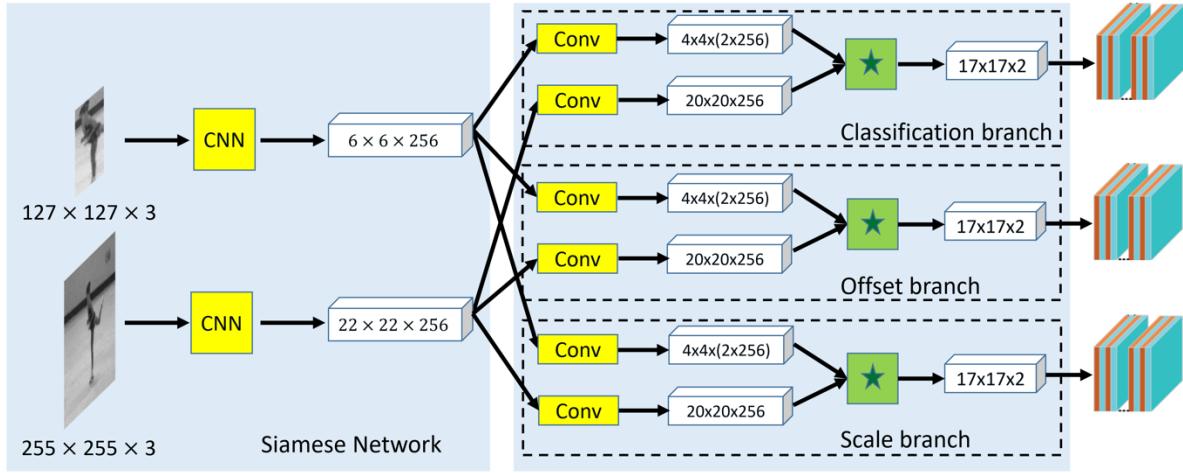
Figure 2. Main framework of Anchor Free Siamese Network (AFSN): On the left is the feature extraction subnetwork. Three branches, namely classification branch, offset branch and scale branch lies in the middle. These three branches are kused for classifying foreground and background, eliminating the deviation and predicting the object size. Then, depth-wise correlation is performed to obtain the final 2-layer score map, 2-layer tracking offset for x and y axis and 2-layer object size: width and height.

trackers are however a bit inefficient.

2.2. Dataset

OTB2015 [42] constructs a benchmark dataset with 100 fully annotated sequences to facilitate the performance evaluation. It is an extension of OTB2013 [41], which contains 50 representative video sequences. The VOT [19, 21, 20] datasets are constructed by a novel video clustering approach based on visual properties. The dataset is fully annotated, all the sequences are labelled per-frame with visual attributes to facilitate in-depth analysis. The OTB [41, 42], ALOV [35] and VOT [19, 21, 20] datasets represent the initial attempts to unify the testing data and performance measurements of generic object tracking. Recently, GOT-10k [17] has been proposed and is larger than most tracking datasets, which offers a much wider coverage of moving object. Several competitive trackers (MDNet [31], SINT [37], GOTURN [13]) are trained on video sequences using OTB and VOT dataset. However, this practice has been prohibited in the VOT challenge. Thus, we train our network with the GOT-10k dataset, which differs from the video sequences in the benchmark. It is less likely for our model to over-fit the scenes and objects in the benchmark.

2.3. Anchor free tracking

Faster RCNN [34] generates region proposal within the detection network. It samples fixed shape anchors on a low resolution image and classifies each into foreground or background. SiamRPN [25] has adopted RPN into tracking scenario. The improved versions of SiamRPN, DaSiamRPN [48] and SiamRPN++ [24] are all successful trackers. However, the enumeration of a nearly exhausted list of anchors is inefficient and requires extra post-processing. The tracking accuracy is also restricted by the pre-proposed fixed shape bounding boxes.

Keypoint estimation has some great applications in detection. CornerNet [23] detects two bounding box corners as keypoints. ExtremeNet [32] predicts the four corners and center points for all objects. CenterNet [47] extracts a single center point per object without the need for post-processing. Since anchor free method solely generates the bounding box once in one inference time, its simplicity can boost the deep learning trackers. Different anchor free trackers represent the object using different techniques. Some represent the four corners, others represent the center point. This provides a variety of opportunities using anchor free in tracking. Anchor free has many successful applications in detection because of its efficiency and great performance. However, it has not been fully exploited in tracking.

3. Siamese tracking without anchors

In this section, we describe the proposed AFSN framework in detail. As shown in Fig. 2, the AFSN consists of a Siamese network for feature extraction. Three branches, namely classification branch, offset branch and scale branch are used for classifying foreground and background, eliminating the deviation and predicting the object size. Image pairs are fed into the proposed framework for end-to-end training.

3.1. Bounding box center

Our aim is to represent the object with the bounding box center. Scales and tracking offset are regressed di-

rectly from image features at the center location. Let $Y \in R^{W \times H \times 3}$ be an output score map of classification branch with width W and height H. Suppose $\hat{Y}_{(x_i, y_j, k)}$ is the value of point (x_i, y_j) on the score map of the kth frame. A prediction $\hat{Y}_{(x_i, y_j, k)} = 1$ corresponds to the tracking object center, while $\hat{Y}_{(x_i, y_j, k)} = 0$ is the background.

The classification labels Y are designed to represent various foreground objects. Therefore, the groundtruth keypoints are designed to obey two-dimension normal distribution. The mean value is the center of bounding box. According to the three sigma rule [33], the probability for X falling away from its mean by more than 3 standard deviation is at most 5% if X obeys the normal distribution. Thus, the standard deviation in our label is one sixth of the width and height:

$$Y = \frac{1}{2\pi\sigma_1\sigma_2} exp \left\{ -\frac{1}{2} \left[\frac{(x - \mu_1)^2}{\sigma_1^2} + \frac{(y - \mu_2)^2}{\sigma_2^2} \right] \right\} \quad (1)$$

The response value intensifies with the increase of overlapping area between the exemplar and the instance. Hence, the score around the edge of bounding box should be lower than the center part.

The training objective is a penalty-reduced pixel-wise logistic regression with focal loss [26]:

$$L_{cls} = -\frac{1}{N} \sum \begin{cases} \left(1 - \hat{Y}_{xyk}\right)^\alpha \log(\hat{Y}_{xyk}) & Y_{xyk} = 1 \\ (1 - Y_{xyk})^\beta \left(\hat{Y}_{xyk}\right)^\alpha & Y_{xyk} = 1, \\ \log(1 - \hat{Y}_{xyk}) \end{cases}$$
$$(2)$$

where α and β are hyper parameters of the focal loss, and N is the number of frames in one epoch. We use $\alpha = 2$ and $\beta = 4$ in all our experiments, following Law and Deng [23].

3.2. Tracking offset

Since the input exemplar size, instance size and the output score map are 127×127, 255×255 and 17×17 separately, the stride of the network is 8. To eliminate the deviation and restore the gap, a tracking offset is added for each point on the score map. For the i th point, tracking offsets $O_k = \left\{ (\delta x_k^{(i)}, \delta y_k^{(i)}) \right\}_{i=1}^n$ can be expressed as:

$$O_k = (x_k/stride - \hat{x}_k, y_k/stride - \hat{y}_k) \quad (3)$$

Then, the offset is trained with the L1 loss L_{off}. Each point on the score map is considered, which assists locating the bounding box even if the center peak deviates from the groundtruth.

3.3. Scale estimation

To estimate the size of an object is equivalent to regress the object size $S_k = (x_{k2} - x_{k1}, y_{k2} - y_{k1})$ in each frame.

To make sure the estimation falls in the positive region, we represent the size with α_k and β_k as:

$$S_k = \left(e^{\alpha_k}, e^{\beta_k}\right) \quad (4)$$

Then, a simple prediction is conducted. The L1 loss for the scale estimation at the bounding box center is:

$$L_{scl} = \frac{1}{N} \sum_k \left[\left|\hat{\alpha}_{P_k} - \alpha_k\right| + \left|\hat{\beta}_{P_k} - \beta_k\right| \right] \quad (5)$$

Keypoint heatmap [2]   Local offset [2]   Object size [2]

Figure 3. The outputs of the proposed anchor free Siamese network: score map, tracking offset and object size.

3.4. Training

The feature extraction subnetwork is fully-convolutional. The search of optimum network architecture is presented in Section 4. Two branches compose the subnetwork. The template branch receives the exemplar patch (denoted as z). The search branch receives the full-scale instance patch (denoted as x). The two feature extraction branches share the same parameters. Thus, the same types of features can be compared in the following network. Let L_t represent the extraction operator $(L_t x)[u] = x[u - t]$, and the definition of fully convolution within stride k can be defined as:

$$h(L_{kt}x) = L_t h(x) \quad (6)$$

Correlation operator is a batch processing function, which compares the Euclidean distance or similarity metric between $\phi(z)$ and $\phi(x)$. Note that $\phi(z)$ and $\phi(x)$ denote the outputs of template and search branches, respectively. Combining deep features in a higher dimension is equivalent to dense sampling around the bounding box and evaluating similarity after each feature extraction. However, the former method is more efficient due to the smaller scale of higher dimension feature. For convenience, let $u(\phi(z), \phi(x))$ denote the output of correlation function.

Since no normalization for offset and scale is included, the overall loss function is:

$$loss = L_{cls} + \lambda_{off}L_{off} + \lambda_{scl}L_{scl}, \quad (7)$$

where λ_{off} and λ_{scl} are two hyper-parameters to balance the three parts. In our experiment, we set $\lambda_{off} = 0.1$ and $\lambda_{scl} = 4$. Only this single network is used to predict the bounding box center $\hat{Y}_k$, tracking offset $\hat{O}_k$ and object size $\hat{S}_k$

AFSN1	AFSN2	AFSN3	AFSN4	AFSN5	AFSN6	AFSN7	AFSN8
$\begin{bmatrix} k11\,s2 & 3 & 96 \\ BN & 96 & 96 \\ ReLU & 96 & 96 \end{bmatrix}$	$\begin{bmatrix} k5\,s2 & 3 & 64 \\ BN & 64 & 64 \\ ReLU & 64 & 64 \end{bmatrix}$	$\begin{bmatrix} k5\,s2 & 3 & 64 \\ BN & 64 & 64 \\ ReLU & 64 & 64 \end{bmatrix}$	$\begin{bmatrix} k5\,s2 & 3 & 96 \\ BN & 96 & 96 \\ ReLU & 96 & 96 \end{bmatrix}$	$\begin{bmatrix} k5\,s2 & 3 & 96 \\ BN & 96 & 96 \\ ReLU & 96 & 96 \end{bmatrix}$	$\begin{bmatrix} k5\,s2 & 3 & 96 \\ BN & 96 & 96 \\ ReLU & 96 & 96 \end{bmatrix}$ $\begin{bmatrix} k3\,s1 & 96 & 128 \\ BN & 128 & 128 \\ ReLU & 128 & 128 \end{bmatrix}$ $\begin{bmatrix} k3\,s1 & 128 & 128 \\ BN & 128 & 128 \\ ReLU & 128 & 128 \end{bmatrix}$	$\begin{bmatrix} k5\,s2 & 3 & 96 \\ BN & 96 & 96 \\ ReLU & 96 & 96 \end{bmatrix}$	$\begin{bmatrix} k5\,s2 & 3 & 96 \\ BN & 96 & 96 \\ ReLU & 96 & 96 \end{bmatrix}$
[$MaxPool(k3,s2)$]	[$MaxPool(k3,s2)$]	[$MaxPool(k3,s2)$]	[$MaxPool(k3,s2)$]	[$MaxPool(k3,s2)$]	[$MaxPool(k3,s2)$]	[$MaxPool(k3,s2)$]	[$MaxPool(k3,s2)$]
$\begin{bmatrix} k5\,s1 & 96 & 256 \\ BN & 256 & 256 \\ ReLU & 256 & 256 \end{bmatrix}$ $group=2$	$\begin{bmatrix} k5\,s1 & 64 & 128 \\ BN & 128 & 128 \\ ReLU & 128 & 128 \end{bmatrix}$	$\begin{bmatrix} k5\,s1 & 64 & 128 \\ BN & 128 & 128 \\ ReLU & 128 & 128 \end{bmatrix}$	$\begin{bmatrix} k3\,s1 & 96 & 256 \\ BN & 256 & 256 \\ ReLU & 256 & 256 \end{bmatrix}$ $group=2$	$\begin{bmatrix} k5\,s1 & 96 & 256 \\ BN & 256 & 256 \\ ReLU & 256 & 256 \end{bmatrix}$ $group=2$	$\begin{bmatrix} k3\,s1 & 128 & 256 \\ BN & 256 & 256 \\ ReLU & 256 & 256 \end{bmatrix}$ $group=2$	$\begin{bmatrix} k3\,s1 & 96 & 256 \\ BN & 256 & 256 \\ ReLU & 256 & 256 \end{bmatrix}$	$\begin{bmatrix} k3\,s1 & 96 & 256 \\ BN & 256 & 256 \\ ReLU & 256 & 256 \end{bmatrix}$ $group=2$ $\begin{bmatrix} k3\,s1 & 256 & 256 \\ BN & 256 & 256 \\ ReLU & 256 & 256 \end{bmatrix}$ $group=2$
[$MaxPool(k3,s2)$]	[$MaxPool(k3,s2)$]	[$MaxPool(k3,s2)$]	[$MaxPool(k3,s2)$]	[$MaxPool(k3,s2)$]	[$MaxPool(k3,s2)$]	[$MaxPool(k3,s2)$]	[$MaxPool(k3,s2)$]
$\begin{bmatrix} k3\,s1 & 256 & 384 \\ BN & 384 & 384 \\ ReLU & 384 & 384 \end{bmatrix}$ $\begin{bmatrix} k3\,s1 & 384 & 384 \\ BN & 384 & 384 \\ ReLU & 384 & 384 \end{bmatrix}$ $group=2$	$\begin{bmatrix} k3\,s1 & 128 & 256 \\ BN & 256 & 256 \\ ReLU & 256 & 256 \end{bmatrix}$ $\begin{bmatrix} k3\,s1 & 256 & 256 \\ BN & 256 & 256 \\ ReLU & 256 & 256 \end{bmatrix}$ $group=2$	$\begin{bmatrix} k5\,s1 & 128 & 256 \\ BN & 256 & 256 \\ ReLU & 256 & 256 \end{bmatrix}$ $\begin{bmatrix} k5\,s1 & 256 & 256 \\ BN & 256 & 256 \\ ReLU & 256 & 256 \end{bmatrix}$	$\begin{bmatrix} k3\,s1 & 256 & 384 \\ BN & 384 & 384 \\ ReLU & 384 & 384 \end{bmatrix}$ $\begin{bmatrix} k3\,s1 & 384 & 384 \\ BN & 384 & 384 \\ ReLU & 384 & 384 \end{bmatrix}$ $group=2$	$\begin{bmatrix} k3\,s1 & 256 & 256 \\ BN & 384 & 384 \\ ReLU & 256 & 256 \end{bmatrix}$ $\begin{bmatrix} k3\,s1 & 256 & 256 \\ BN & 384 & 384 \\ ReLU & 256 & 256 \end{bmatrix}$ $group=2$	$\begin{bmatrix} k3\,s1 & 256 & 256 \\ BN & 384 & 384 \\ ReLU & 256 & 256 \end{bmatrix}$ $\begin{bmatrix} k3\,s1 & 256 & 256 \\ BN & 384 & 384 \\ ReLU & 256 & 256 \end{bmatrix}$ $group=2$	$\begin{bmatrix} k3\,s1 & 256 & 384 \\ BN & 384 & 384 \\ ReLU & 384 & 384 \end{bmatrix}$ $\begin{bmatrix} k3\,s1 & 384 & 384 \\ BN & 384 & 384 \\ ReLU & 384 & 384 \end{bmatrix}$	$\begin{bmatrix} k3\,s1 & 256 & 384 \\ BN & 384 & 384 \\ ReLU & 384 & 384 \end{bmatrix}$ $\begin{bmatrix} k3\,s1 & 384 & 384 \\ BN & 384 & 384 \\ ReLU & 384 & 384 \end{bmatrix}$ $group=2$
$[k3\,s1 \quad 384 \quad 256]$ $group=2$	$[k3\,s1 \quad 256 \quad 128]$	$[k3\,s1 \quad 256 \quad 128]$	$[k3\,s1 \quad 384 \quad 256]$ $group=2$	$[k3\,s1 \quad 256 \quad 256]$ $group=2$	$\begin{bmatrix} k3\,s1 & 256 & 256 \\ BN & 256 & 256 \\ ReLU & 256 & 256 \end{bmatrix}$ $group=2$	$[k3\,s1 \quad 384 \quad 256]$	$[k3\,s1 \quad 384 \quad 256]$ $group=2$
0.599	0.567	0.493	0.638	0.588	0.319	0.612	0.593

Figure 4. Architectures of designed backbone networks for AFSN. In this architecture list, k is the kernel size, s is the general convolution stride and $group$ is the number of group convolution. on the bottom is the success rate tested on OTB2015 benchmark.

3.5. Tracking

At inference time, the points with the highest response score are extracted in the score map. In order to avoid noises or sudden changes in the background, we also apply a hanning window on the final score map. Suppose $\hat{P}_k = (\hat{x}_k, \hat{y}_k)$ is the predicted center point in the k th frame. Combining the regressed tracking offset $\hat{O}_k = (\delta\hat{x}_k, \delta\hat{y}_k)$ and the object size $\hat{S}_k = (\hat{w}_k, \hat{h}_k)$, the estimated bounding box can be expressed as:

$$\left(\hat{x}_k + \delta\hat{x}_k - \hat{w}_k/2, \hat{y}_k + \delta\hat{y}_k - \hat{h}_k/2, \hat{w}_k, \hat{h}_k\right) \quad (8)$$

A more explicit way of illustrating the Siamese output is shown in Figure 3.

4. Network backbone

This section presents the process of optimizing the network backbone for the proposed AFSN tracker. Stride, receptive field, group convolution and kernel size are the impact factors of different networks. For a faster network searching process, the backbone networks are trained by 40% GOT-10k dataset [17] with 20 epochs.

With the size of the input image and output score map, the stride of Siamese trackers can be calculated as:

$$\frac{instance - exemplar}{scoremap - 1} = stride \quad (9)$$

The aggregation of different kernel size controls the region of the receptive field. A larger receptive field provides greater image context, but shallow features like color, shape will be lost. A smaller receptive field focuses on several particular parts on objects, but it cannot capture the structure of target objects. From Eq. 9, we can find that if we increase the receptive field, the score map size will decrease because more information are contained in one convolution. Then, the stride will increase, leading to a larger gap between two exemplar images. The final tracking results are generally correct around the target object, but the accurate localization and scale estimation cannot be achieved. If the receptive field decreases in order to capture the detail features, the gap will also decrease. However, once the bounding box deviates from the tracking object, it shows less robustness to relocate the object. Although the predicted scale will be more accurate in this scenario, the accuracy will not increase due to the poor robustness, In Siamese tracking, template image is not updated online, which further decreases the accuracy. This is a common contradictory in Siamese network, and it also explains why the backbone networks in Siamese trackers are relatively shallow.

To optimize and search for the best backbone network, 8 different backbones are trained as shown in Fig. 4. Network stride affects the overlap area of receptive fields for two neighboring output score maps. The proposed AFSN prefers a relatively small network stride, which is around 7 to 9 (AFSN1 *vs.* AFSN6 *vs.* AFSN8). In these cases, the

5

depth of the shallow layers largely affect the success rate. Since shallow features like color and shape can be applied on several similar background objects, there is no need to extract more shallow features. Therefore, the receptive field is better set at 70% to 80% of the exemplar image. Group convolution separates different channels to different kernels, which increases the robustness of the tracking (ASFN4 *vs.* AFSN7). It also decreases the computation amount. More channel numbers extract more features and offer more similarity information to compare, the optimum channel numbers for deeper layers is 256 (AFSN1 *vs.* AFSN2 *vs.* AFSN3).

5. Experiments

This section presents the results of our anchor free Siamese network on five challenging tracking datasets, *i.e.*, OTB2015, VOT2015, VOT2016, VOT2018 and TrackingNet. All the tracking results are compared with the state-of-the-art trackers using the reported results to ensure a fair comparison.

5.1. Implementation details

The parameters in the proposed AFSN are trained from scratch, and the overall training objective optimizes the loss function in Eq. 7 with SGD. There are totally 50 epochs conducted and the learning rate decreases in the log space from 10^{-3} to 10^{-6}. Since the loss in tracking offset occupies most of the loss in the first phase of training, we set a cut off at 10^{-8} for the offset loss. We extract image pairs from GOT-10k dataset for training and test on OTB and VOT dataset to verify the feasibility and efficiency of our model. The template image is cropped centering on the foreground object with size of $A \times A$:

$$(w + p) \times (h + p) = A^2, \tag{10}$$

where w, h are the target bounding box width and height and $p = \frac{w+h}{2}$. For the template branch, A is 127, and for the instance branch, A is 255.

5.2. Ablation experiments

To investigate the impact of anchor free method, we change the training label for SiamFC and SiamRPN without changing the input and hyper-parameters of the original models. SiamFC finds the best tracking scale by enumerating three potential ratio: $1.025^{-1,0,1}$. We represent it with a new score map following the two-dimension normal distribution. The size can be directly predicted according to the response. Through combining the original model with the newly designed label, the precision rate and the success rate on OTB2015 grow 7.65% and 5.15%, as shown in Fig. 5 and 6. We also apply this approach to SiamRPN. The precision rate drop a little, mainly because the tracking offset is

not included. The position estimation may drift caused by the locations of the pre-proposed anchors. Even though no offset is incorporated, the success rate increases 3.14%. The results demonstrate that the anchor free design can improve the tracking performance.
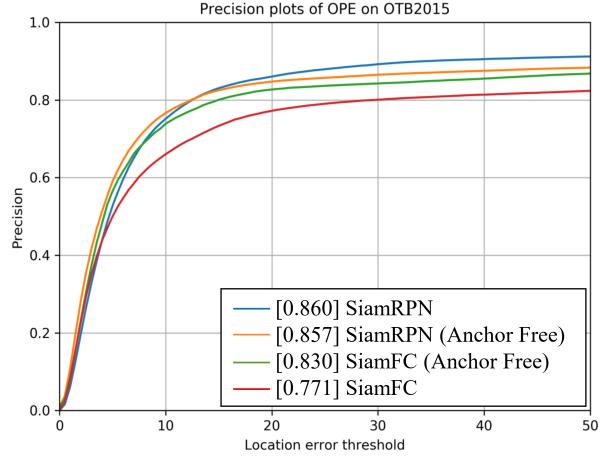
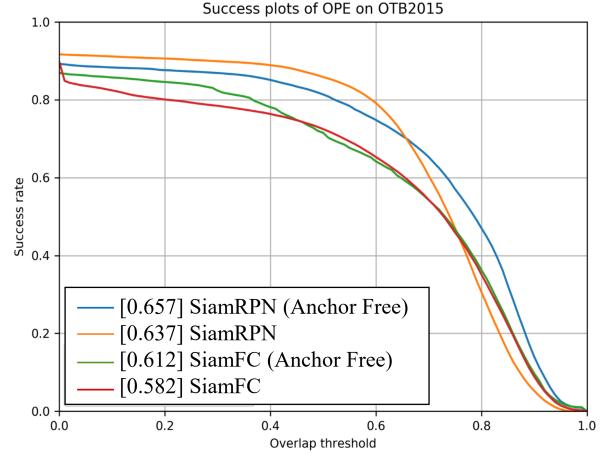Figure 5. Ablation experiments: precision plot on OTB2015

Figure 6. Ablation experiments: success plot on OTB2015

5.3. Results on OTB2015

OTB-2015 Benchmark The standardized OTB benchmark provides a fair test for both accuracy and robustness. The benchmark [42] considers the precision plot and the success plot of one path evaluation (OPE). The precision plot considers the percentage of frames in which the estimated locations are within a given threshold distance of the target bounding box. The definition of average success rate is that a tracker is successful in a given frame if the intersection-over-union between its estimation and the

groundtruth is above a certain threshold.

We compare our anchor free Siamese tracker on the OTB2015 with the state-of-the-art trackers including SiamRPN [25], ACFN [6], Staple [3],SiamFC [4], CNN-SVM [16], DSST [7], CF2 [36], MOSSE [5], KCF [15], CSK [14]. Fig. 7 and 8 show that our tracker produces leading results. Compared with the recent SiamRPN [25], the precision rate and success rate increase 0.93% and 5.97%, respectively.
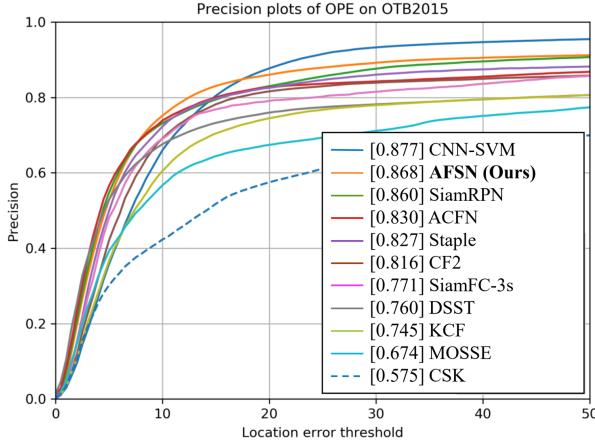

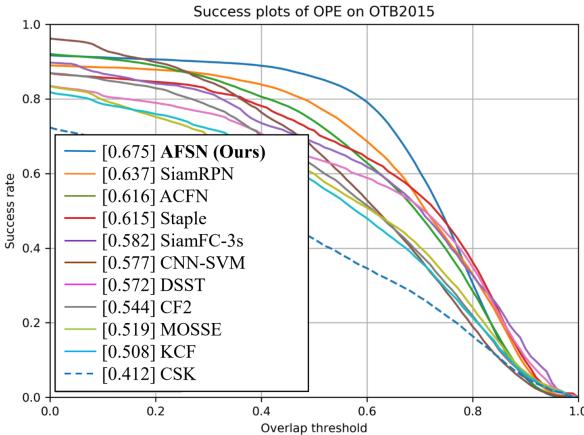Figure 7. Precision plot of OTB2015

Figure 8. Success plot of OTB2015

5.4. Results on VOT2015

The VOT2015 dataset consists on 60 sequences [22]. The overall performance is evaluated using Expected Average Overlap (EAO), which takes account of both accuracy and robustness. Besides, the speed is evaluated with a normalized speed Equivalent Filter Operations (EFO).

We compared our AFSN with 10 state-of-the-art trackers. The results are reported in Tab. 1. SiamFC and

SiamRPN are added into comparisons as our baselines. As is shown in Fig. 9, our tracker is able to rank the 1st in EAO. SiamFC is one of the top trackers on VOT2015 which can run at frame rates beyond real time and achieves state-of-the-art performance. SiamRPN is able to gain 23% increase in EAO, and our AFSN can achieve 0.381 in EAO, which is 9.2% higher than SiamRPN. Also, AFSN is able to rank the 1st in accuracy, the 2nd in EFO and the 3rd in failure.
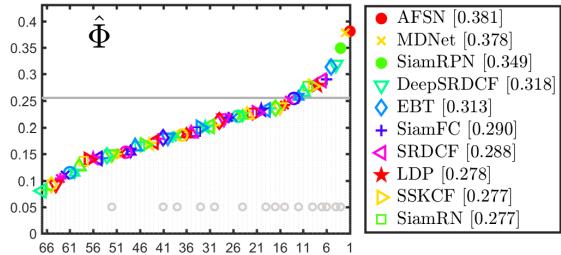

Figure 9. EAO scores rank on VOT2015

Table 1. Results about the state-of-the-art trackers in VOT2015. Red, blue and green represent the 1st, 2nd and 3rd respectively.

Tracker	EAO	Accuracy	Failure	EFO
DeepSRDCF	0.3181	0.56	1.0	0.38
EBT	0.313	0.45	1.02	1.76
SRDCF	0.2877	0.55	1.18	1.99
LDP	0.2785	0.49	1.3	4.36
sPST	0.2767	0.54	1.42	1.01
SC-EBT	0.2548	0.54	1.72	0.8
NSAMF	0.2536	0.53	1.29	5.47
Struck	0.2458	0.46	1.5	2.44
RAJSSC	0.242	0.57	1.75	2.12
S3Tracker	0.2403	0.52	1.67	14.27
SiamFC-3s	0.2904	0.54	1.42	8.68
SiamRPN	0.349	0.58	0.93	23.0
AFSN	0.381	0.59	1.01	20.4

5.5. Results on VOT2016

The video sequences in VOT2016 are the same as VOT2015, but the groundtruth bounding boxes are re-annotated. We compare our trackers to the top 20 trackers in the challenge. As shown in Fig. 10, AFSN can outperform all entries in challenge. Tab. 2 shows the information of several state-of-the-art trackers. AFSN can achieve a 12.4% gain in EAO, 15.1% in accuracy compared with C-COT [8]. Our tracker also outperforms SiamRPN in EAO, accuracy and failure. Most prominently, Our tracker operates at 136 FPS, which is $425\times$ faster than C-COT.
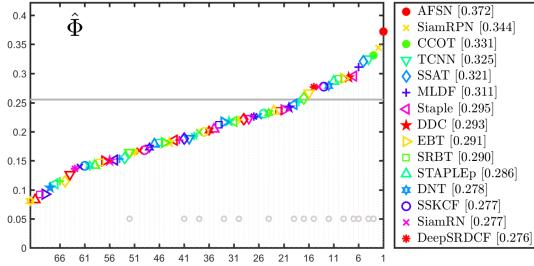
7

Figure 10. Expected overlap scores in the VOT2016 challenge.

Table 2. Results about the published state-of-the-art trackers in VOT2016. Red, blue and green represent the 1st, 2nd and 3rd respectively.

Tracker	EAO	Accuracy	Failure	EFO
C-COT	0.331	0.53	0.85	0.507
ECO-HC	0.322	0.53	1.08	15.13
Staple	0.2952	0.54	1.35	11.14
EBT	0.2913	0.47	0.9	3.011
MDNet	0.257	0.54	1.2	0.534
SiamRN	0.2766	0.55	1.37	5.44
SiamAN	0.2352	0.53	1.65	9.21
SiamRPN	0.3441	0.56	1.08	23.3
AFSN	0.372	0.61	1.04	20.6

5.6. Results on VOT2018

VOT2018 [20] dataset consists of 60 video sequences. The performance is also evaluated in terms of accuracy (average overlap in the course of successful tracking) and robustness (failure rate). EAO is the combination of these two measurements. Tab. 4 shows the comparison of our approach with the top 10 trackers in the VOT2018 challenge. Among the top trackers, our AFSN achieves the best EAO and accuracy, while having competitive robustness. Although recently released SiamRPN++ [24] can achieve 0.414 in EAO, our AFSN can operate at $3.9\times$ faster (136 FPS *v.s.* 35 FPS) than SiamRPN++ with only a 4% drop in EAO.
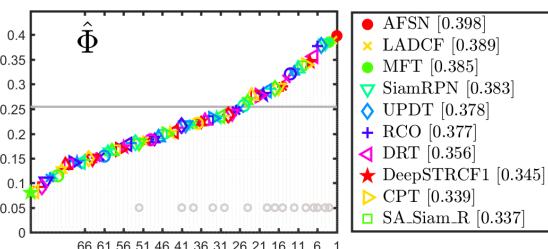

Figure 11. EAO scores rank on VOT2018

Table 3. Results about the published state-of-the-art trackers in VOT2018. Red, blue and green represent the 1st, 2nd and 3rd respectively.

Tracker	EAO	Accuracy	Robustness
LADCF	0.389	0.503	0.159
MFT	0.385	0.505	0.140
DaSiamRPN	0.383	0.586	0.276
UPDT	0.378	0.536	0.184
RCO	0.376	0.507	0.155
DRT	0.356	0.519	0.201
DeepSTRCF	0.345	0.523	0.215
CPT	0.339	0.506	0.239
SASiamR	0.337	0.566	0.258
DLSTpp	0.325	0.543	0.224
AFSN	0.398	0.589	0.204

5.7. Results on TrackingNet

TrackingNet [30] is the first large-scale dataset and benchmark for object tracking in the wild. It provides more than 30K videos with more than 14 million dense bounding box annotations sampled from YouTube. The dataset covers a wide selection of object classes in broad and diverse context. The trackers are evaluated using an online evaluation server on a test set of 511 videos. The results of precision, normalized precision and success are reported in Tab. 4. MDNet achieves scores of 0.565 and UPDT achieves 0.611 in terms of precision and success, respectively. Our AFSN ranks the 1st with relative gains of 7.4% and 7.2%.

Table 4. Comparison pn the TrackingNet test set with the state-of-the-art trackers. Red, blue and green represent the 1st, 2nd and 3rd respectively.

Tracker	Precision	Norm precision	Success
UPDT	0.557	0.702	0.611
MDNet	0.565	0.705	0.606
CFNet	0.533	0.654	0.578
SiamFC	0.533	0.666	0.571
DaSiamRPN	0.413	0.602	0.568
ECO	0.492	0.618	0.554
CSRDCF	0.480	0.622	0.534
SAMF	0.477	0.598	0.504
Staple	0.470	0.603	0.528
AFSN	0.607	0.738	0.655

6. Conclusions

This paper presents the first in-depth study on anchor free object tracking called Anchor Free Siamese Network (AFSN). Unlike traditional Siamese trackers, the proposed AFSN does not need to enumerate an exhaustive list of potential object locations and classify each anchor. A target object is characterized by a bounding box center, tracking

offset and object size. All three are regressed by Siamese network, performed one time per frame. We also optimize Siamese network architecture for AFSN, and perform extensive ablation experiments to quantitatively illustrate effectiveness of AFSN. We evaluate AFSN using five most commonly used benchmarks and compare to the best anchor-based trackers with source codes available for each benchmark. AFSN is $3 \times -425 \times$ faster than these best anchor based trackers. AFSN is also 5.97% to 12.4% more accurate in terms of all metrics for benchmark sets OTB2015, VOT2015, VOT2016, VOT2018 and TrackingNet, except that SiamRPN++ is 4% better than AFSN in terms of Expected Average Overlap (EAO) on VOT2018 (but SiamRPN++ is $3.9 \times$ slower).

References

[1] S. Avidan. Support vector tracking. *IEEE Transactions on Pattern Analysis and Machine Intelligence*, 26(8):1064–1072, Aug 2004.

[2] S. Avidan. Ensemble tracking. *IEEE Transactions on Pattern Analysis and Machine Intelligence*, 29(2):261–271, Feb 2007.

[3] L. Bertinetto, J. Valmadre, S. Golodetz, O. Miksik, and P. H. Torr. Staple: Complementary learners for real-time tracking. In *The IEEE Conference on Computer Vision and Pattern Recognition (CVPR)*, June 2016.

[4] L. Bertinetto, J. Valmadre, J. F. Henriques, A. Vedaldi, and P. H. Torr. Fully-convolutional siamese networks for object tracking. In *Computer Vision – ECCV 2016 Workshops*, pages 850–865, Cham, 2016. Springer International Publishing.

[5] D. Bolme, J. Beveridge, B. Draper, and Y. Lui. Visual object tracking using adaptive correlation filters. pages 2544–2550, 06 2010.

[6] J. Choi, H. J. Chang, S. Yun, T. Fischer, Y. Demiris, and J. Y. Choi. Attentional correlation filter network for adaptive visual tracking. In *2017 IEEE Conference on Computer Vision and Pattern Recognition (CVPR)*, pages 4828–4837, July 2017.

[7] M. Danelljan, G. Hger, and F. Khan. Accurate scale estimation for robust visual tracking. *British Machine Vision Conference*, pages 1–11, 01 2014.

[8] M. Danelljan, A. Robinson, F. Khan, and M. Felsberg. Beyond correlation filters: Learning continuous convolution operators for visual tracking. volume 9909, pages 472–488, 10 2016.

[9] J. Doellinger, V. S. Prabhakaran, L. Fu, and M. Spies. Environment-aware multi-target tracking of pedestrians. *IEEE Robotics and Automation Letters*, 4(2):1831–1837, April 2019.

[10] H. Grabner, M. Grabner, and H. Bischof. Real-time tracking via on-line boosting. volume 1, pages 47–56, 01 2006.

[11] Q. Guo, W. Feng, C. Zhou, R. Huang, L. Wan, and S. Wang. Learning dynamic siamese network for visual object tracking. In *2017 IEEE International Conference on Computer Vision (ICCV)*, pages 1781–1789, Oct 2017.

[12] S. Hare, A. Saffari, and P. H. S. Torr. Struck: Structured output tracking with kernels. In *2011 International Conference on Computer Vision*, pages 263–270, Nov 2011.

[13] D. Held, S. Thrun, and S. Savarese. Learning to track at 100 fps with deep regression networks. In Bastian Leibe, Jiri Matas, Nicu Sebe, and Max Welling, editors, *Computer Vision – ECCV 2016*, pages 749–765, Cham, 2016. Springer International Publishing.

[14] J. Henriques, R. Caseiro, P. Martins, and J. Batista. Exploiting the circulant structure of tracking-by-detection with kernels. volume 7575, pages 702–715, 10 2012.

[15] J. F. Henriques, R. Caseiro, P. Martins, and J. Batista. High-speed tracking with kernelized correlation filters. *IEEE Transactions on Pattern Analysis and Machine Intelligence*, 37(3):583–596, March 2015.

[16] S. Hong, T. You, S. Kwak, and B. Han. Online tracking by learning discriminative saliency map with convolutional neural network. In *Proceedings of the 32Nd International Conference on International Conference on Machine Learning - Volume 37*, ICML'15, pages 597–606. JMLR.org, 2015.

[17] L.H. Huang, X. Zhao, and K.Q. Huang. Got-10k: A large high-diversity benchmark for generic object tracking in the wild. *ArXiv*, abs/1810.11981, 2018.

[18] X. Jia, H. Lu, and M. Yang. Visual tracking via adaptive structural local sparse appearance model. In *2012 IEEE Conference on Computer Vision and Pattern Recognition*, pages 1822–1829, June 2012.

[19] M. Kristan, A. Leonardis, J. Matas, M. Felsberg, R. Pflugfelder, and L. Čehovin. The visual object tracking vot2016 challenge results. In *Computer Vision – ECCV 2016 Workshops*, pages 777–823, Cham, 2016. Springer International Publishing.

[20] M. Kristan, A. Leonardis, J. Matas, M. Felsberg, R. Pflugfelder, L. Zajc, T. Vojir, G. Bhat, and A. Lukežič. The sixth visual object tracking vot2018 challenge results. In *Computer Vision – ECCV 2018 Workshops*, pages 3–53, Cham, 2019. Springer International Publishing.

[21] M. Kristan, A. Leonardis, J. Matas, M. Felsberg, R. Pflugfelder, L. C. Zajc, T. Vojr, G. Hger, A. Lukeic, A. Eldesokey, G. Fernndez, and . Garca-Martn. The visual object tracking vot2017 challenge results. In *2017 IEEE International Conference on Computer Vision Workshops (ICCVW)*, pages 1949–1972, Oct 2017.

[22] M. Kristan, J. Matas, A. Leonardis, M. Felsberg, L. Cehovin, G. Fernandez, T. Vojir, G. Hager, G. Nebehay, and R. Pflugfelder. The visual object tracking vot2015 challenge results. In *The IEEE International Conference on Computer Vision (ICCV) Workshops*, December 2015.

[23] H. Law and J. Deng. Cornernet: Detecting objects as paired keypoints. *International Journal of Computer Vision*, Aug 2019.

[24] B. Li, W. Wu, Q. Wang, F.Y. Zhang, J.L. Xing, and J.J. Yan. Siamrpn++: Evolution of siamese visual tracking with very deep networks. *CoRR*, abs/1812.11703, 2018.

[25] B. Li, J.J. Yan, W. Wu, Z. Zhu, and X.L. Hu. High performance visual tracking with siamese region proposal network. In *The IEEE Conference on Computer Vision and Pattern Recognition (CVPR)*, June 2018.

[26] T.Y. Lin, P. Goyal, R. Girshick, K.M. He, and P. Dollar. Focal loss for dense object detection. In *The IEEE International Conference on Computer Vision (ICCV)*, Oct 2017.

[27] X.C. Liu, H.D. Ma, and S.Q. Li. Pvss: A progressive vehicle search system for video surveillance networks. *Journal of Computer Science and Technology*, 34(3):634–644, May 2019.

[28] X. Mei and H.B. Ling. Robust visual tracking using l(1) minimization. pages 1436 – 1443, 11 2009.

[29] X. Mei, H.B. Ling, Y. Wu, E. Blasch, and l. Bai. Minimum error bounded efficient l1 tracker with occlusion detection (preprint). pages 1257–1264, 06 2011.

[30] M. Muller, A. Bibi, S. Giancola, S. Alsubaihi, and B. Ghanem. Trackingnet: A large-scale dataset and benchmark for object tracking in the wild. In *The European Conference on Computer Vision (ECCV)*, September 2018.

[31] H. Nam and B. Han. Learning multi-domain convolutional neural networks for visual tracking. In *2016 IEEE Conference on Computer Vision and Pattern Recognition (CVPR)*, pages 4293–4302, June 2016.

[32] F. Nasse and G. A. Fink. A bottom-up approach for learning visual object detection models from unreliable sources. In Axel Pinz, Thomas Pock, Horst Bischof, and Franz Leberl, editors, *Pattern Recognition*, pages 488–497, Berlin, Heidelberg, 2012. Springer Berlin Heidelberg.

[33] F. Pukelsheim. The three sigma rule. *The American Statistician*, 48(2):88–91, 1994.

[34] S.Q. Ren, K.M. He, R. Girshick, and J. Sun. Faster r-cnn: Towards real-time object detection with region proposal networks. In C. Cortes, N. D. Lawrence, D. D. Lee, M. Sugiyama, and R. Garnett, editors, *Advances in Neural Information Processing Systems 28*, pages 91–99. Curran Associates, Inc., 2015.

[35] A. W. M. Smeulders, D. M. Chu, R. Cucchiara, S. Calderara, A. Dehghan, and M. Shah. Visual tracking: An experimental survey. *IEEE Transactions on Pattern Analysis and Machine Intelligence*, 36(7):1442–1468, July 2014.

[36] C. Sun, D. Wang, H.C. Lu, and M.H. Yang. Correlation tracking via joint discrimination and reliability learning. 04 2018.

[37] R. Tao, E. Gavves, and A. Smeulders. Siamese instance search for tracking. pages 1420–1429, 06 2016.

[38] D. Wang, H. Lu, and M. Yang. Online object tracking with sparse prototypes. *IEEE Transactions on Image Processing*, 22(1):314–325, Jan 2013.

[39] Q. Wang, Z. Teng, J. Xing, J. Gao, W. Hu, and S. Maybank. Learning attentions: Residual attentional siamese network for high performance online visual tracking. In *2018 IEEE/CVF Conference on Computer Vision and Pattern Recognition*, pages 4854–4863, June 2018.

[40] Q. Wang, M.D. Zhang, J.L. Xing, J. Gao, W.M. Hu, and Steve M. Do not lose the details: Reinforced representation learning for high performance visual tracking. In *Proceedings of the Twenty-Seventh International Joint Conference on Artificial Intelligence, IJCAI-18*, pages 985–991. International Joint Conferences on Artificial Intelligence Organization, 7 2018.

[41] Y. Wu, J. Lim, and M.H. Yang. Online object tracking: A benchmark. In *The IEEE Conference on Computer Vision and Pattern Recognition (CVPR)*, June 2013.

[42] Y. Wu, J. Lim, and M. Yang. Object tracking benchmark. *IEEE Transactions on Pattern Analysis and Machine Intelligence*, 37(9):1834–1848, Sep. 2015.

[43] X. C. Zhang, P. Ye, S. Y. Peng, J. Liu, K. Gong, and G. Xiao. Siamft: An rgb-infrared fusion tracking method via fully convolutional siamese networks. *IEEE Access*, 7:122122–122133, 2019.

[44] X. C. Zhang, P. Ye, S. Y. Peng, J. Liu, and G. Xiao. Dsiammft: An rgb-t fusion tracking method via dynamic siamese networks using multi-layer feature fusion. *Signal Processing: Image Communication*, 84:115756, 2020.

[45] Z.P. Zhang, H.W. Peng, and Q. Wang. Deeper and wider siamese networks for real-time visual tracking. *CoRR*, abs/1901.01660, 2019.

[46] W. Zhong, H. Lu, and M. Yang. Robust object tracking via sparse collaborative appearance model. *IEEE Transactions on Image Processing*, 23(5):2356–2368, May 2014.

[47] X.Y. Zhou, D.Q. Wang, and P. Krähenbühl. Objects as points. *CoRR*, abs/1904.07850, 2019.

[48] Z. Zhu, Q. Wang, B. Li, W. Wu, J.J. Yan, and W.M. Hu. Distractor-aware siamese networks for visual object tracking. In *The European Conference on Computer Vision (ECCV)*, September 2018.